

Biophysical Journal, Volume 99

**Supporting Material**

**The stepping pattern of myosin X is adapted for processive motility on bundled actin**

Benjamin L Ricca and Ronald Rock

## **SUPPORTING MATERIAL**

**Document S1.** Ten figures and one movie caption.

**The stepping pattern of myosin X is adapted for processive motility on bundled actin**

Benjamin L. Ricca & Ronald S. Rock\*

*Department of Biochemistry and Molecular Biology,  
The University of Chicago, Chicago, Illinois 60637*

\*Author to whom correspondence should be addressed

Ronald S. Rock  
The University of Chicago  
GCIS W240  
929 E 57<sup>th</sup> St.  
Chicago, IL 60637

rrock@uchicago.edu  
+1 773.702.0716

Figure S1

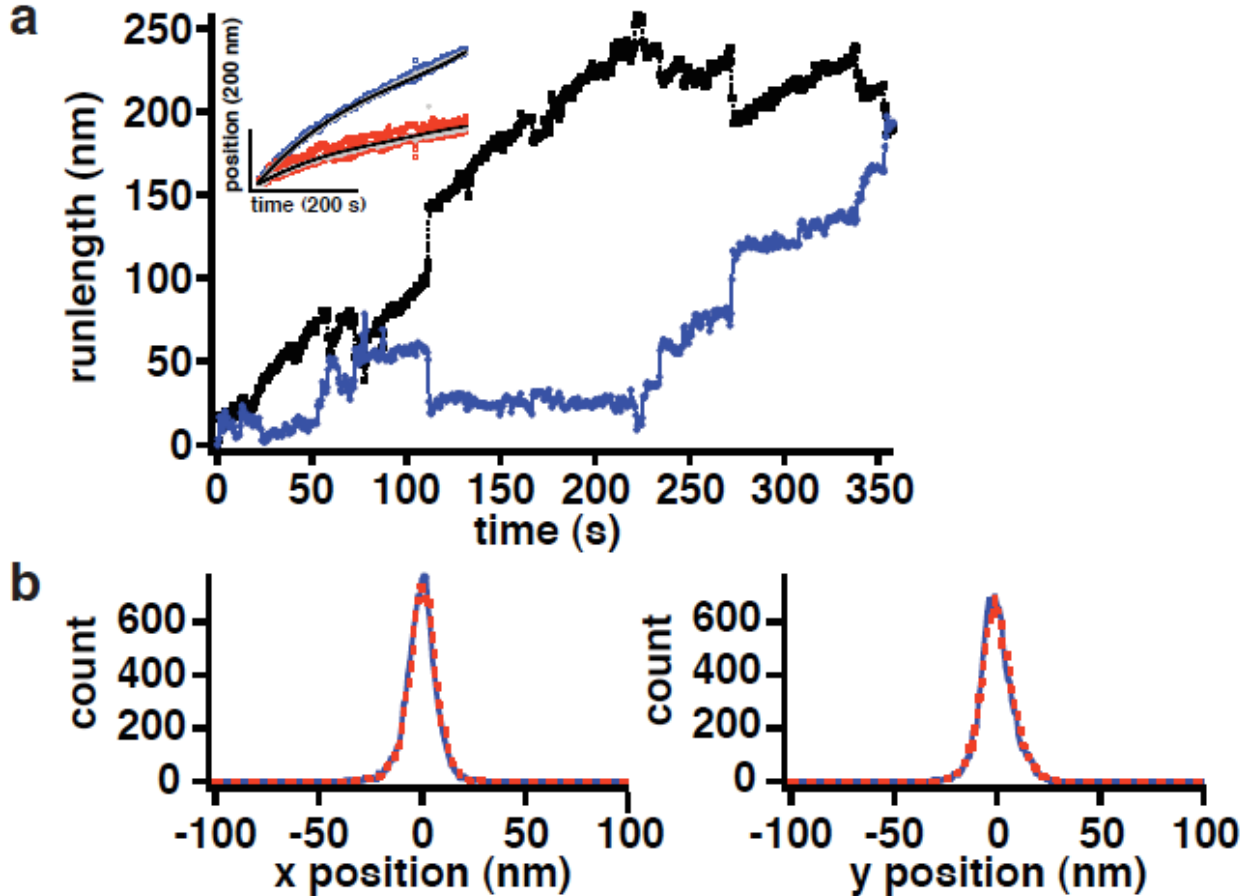


FIGURE S1 For each recorded movie, Qdots stuck to the coverslip surface were used to correct for stage drift. (a) Example of stagedrift correction for one event. Plot of runlength versus time for an example Qdot-labeled motor run before (*black*) and after (*blue*) subtracting the calculated stage drift. (a, *inset*) Refined *x* and *y* positions (*blue* and *red*, respectively) for four Qdots stuck to the coverslip surface in the same movie as the example event. The average *x* and *y* position of the stuck Qdots (a, *inset*, *gray*) through time was fit to a fifth-order polynomial (a, *inset*, *black trace*), which was subtracted from the refined *x* and *y* position data of each motor run along actin from that movie. (b) Histograms of the corrected position of non-moving Qdots. We tested our method of correcting for stage drift on 15 stuck spots from 3 movies (5 spots from each movie). For each spot, the positions of the other four spots in the same movie were used to fit the fifth-order polynomial. The resulting corrected *x* position and (0.00 ± 0.07 nm; mean ± SE) and *y* position (0.00 ± 0.08 nm) are displayed in the histograms (*blue solid traces*; n = 11761 frames). We verified our method by a simple subtraction method. For each spot in each frame, the average displacement from the first frame of the other four stuck spots was subtracted from the spot's current position. The resulting corrected *x* position (0.00 ± 0.07 nm) and *y* position (0.00 ± 0.08 nm) are displayed in the histograms (*red dashed traces*; n = 11761 frames). Agreement between both methods is excellent, but we chose to use the subtraction of the polynomial fit rather than the subtraction of the mean displacement to reduce noise in the correction due to Qdots blinking and the small number of Qdots that remain stuck to the coverslip surface throughout the entirety of a movie.

Figure S2

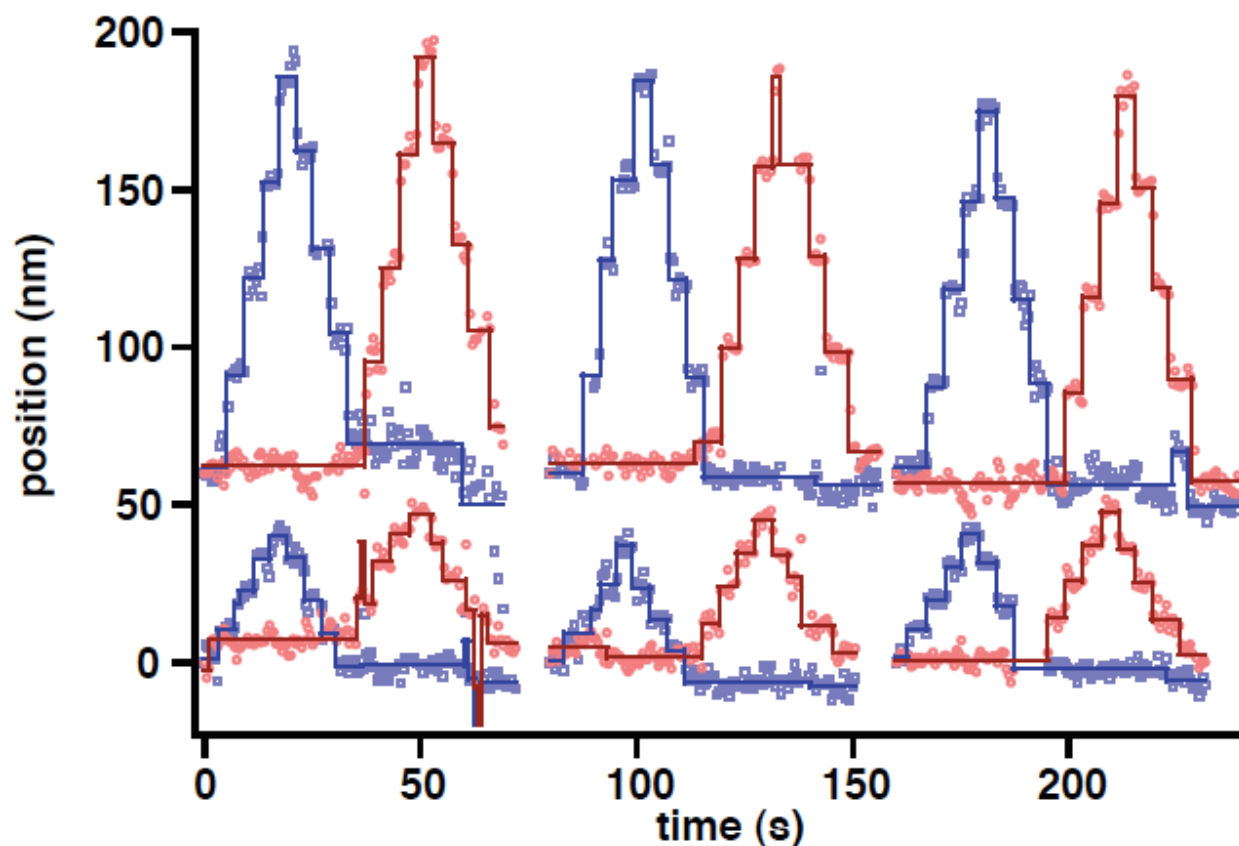


FIGURE S2 Artificial 30 nm and 10 nm steps are well-resolved by FIONA. Six examples of refined position data of surface-attached Qdots moved by stepping the piezo stage in either 30 nm (*top row*) or 10 nm (*bottom row*). The stage was given the following sequence of steps: 4 steps in the positive  $x$  direction, 4 steps in the negative  $x$  direction, 4 steps in the positive  $y$  direction, and 4 steps in the negative  $y$  direction. Refined  $x$  position (*pale blue squares*) and  $y$  position (*pale red circles*) data plotted versus time shows that steps are easily recognizable. The step-fitting algorithm of Kerssemakers, et al. 2006 (2) was used to pick steps (*dark blue and dark red traces*), and the measured stepsizes agree very well with the expected stepsizes,  $29.9 \pm 0.5$  nm ( $n = 64$  steps of 30 nm) and  $10.2 \pm 0.4$  nm ( $n = 63$  steps of 10 nm). Mean and SE for stepsize measurements were calculated as Yildiz et al. 2003 (3). Upon subtraction of the step level fits from the refined position data, we obtain a position measurement of  $0.0 \pm 1.3$  nm (mean  $\pm$  SE,  $n = 7.4$  frames per position from  $>2000$  frames) indicating that our tracking precision is  $<2$  nm.

Figure S3

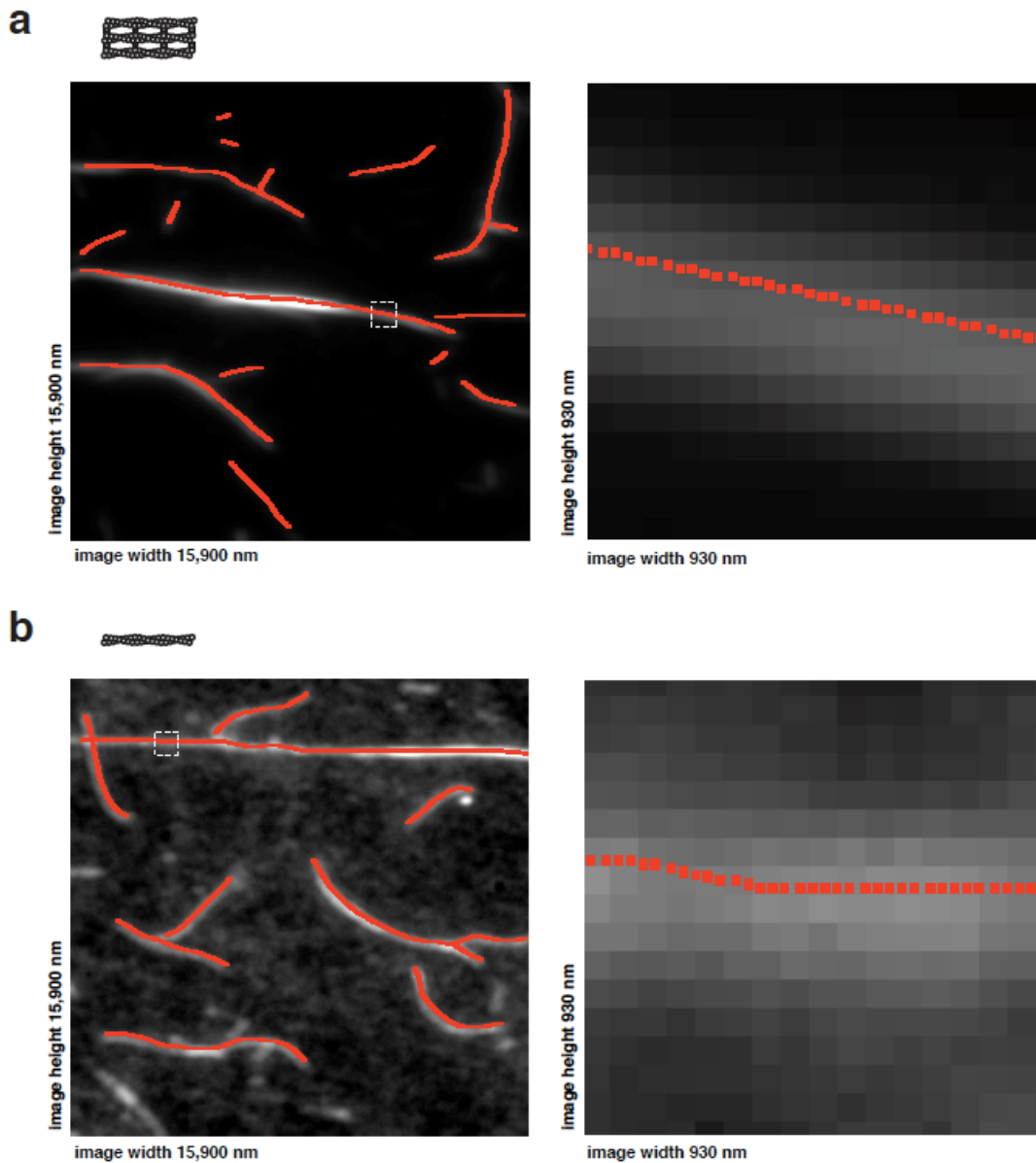


FIGURE S3 The image of actin bundles or actin filaments establishes the position of an axis to describe a myosin motor's run in two dimensions. Selected coordinates describing the actin track (*red*) overlaid on an image of actin bundles (*a*) and on an image of actin filaments (*b*). The region highlighted by the white dashed box for each example is expanded to show the coordinates on a scale in relation to the size of a motor run (100-500 nm). Just prior to imaging Qdot-labeled myosin, an image of the surface attached actin was acquired. Coordinates to describe the position of actin structures were selected from the actin image using the NeuronJ plug-in in ImageJ (1), and additional points were interpolated along the selected actin tracks at half-pixel spacing (~30 nm). Points along an actin track near a motor run were then fit to a line to establish an axis to describe the motor's motion along the length of the actin track. The absolute position of the motor in relation to the established actin axis is not resolvable. However, changes in its position along the length of the actin and perpendicular to the actin are measurable, so we can accurately describe the motor's motion in relation to its actin track.

Figure S4

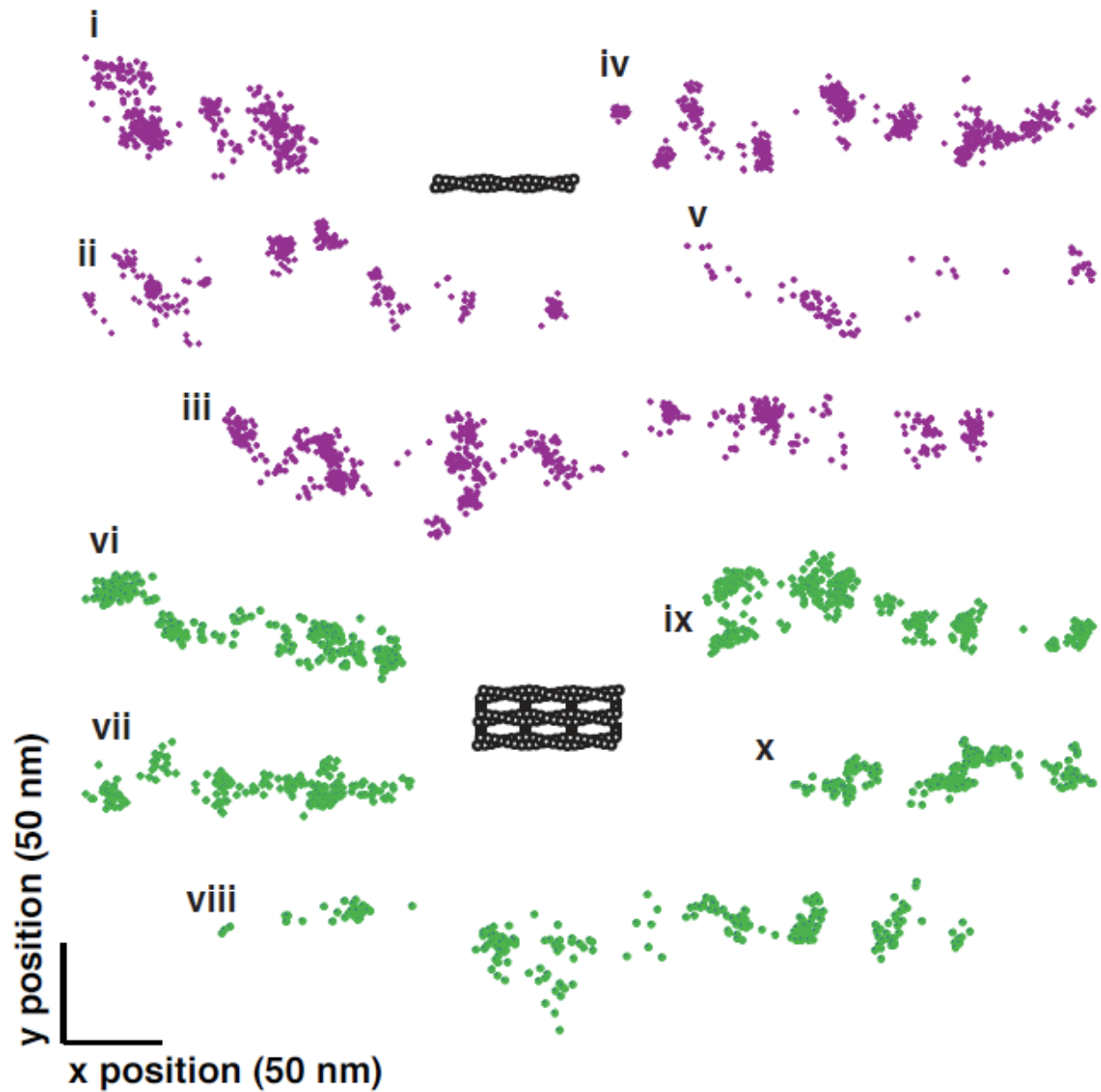


FIGURE S4 Myosin X leans to the right locally as it moves along single actin filaments. Example  $x$  position versus  $y$  position traces of events of Qdot-labeled myosin X as it moves along single actin filaments (*violet, i-v*) and along bundled actin (*green, vi-x*). Each event is labeled near its beginning with a Roman numeral. Events are moving primarily in the positive  $x$  direction. Local clusters of points in events on single actin filaments exhibit a negative slope, while no obvious trend is observed in events on bundled actin. Events (*i*) and (*x*) are the same as those shown in Fig. 3.

Figure S5

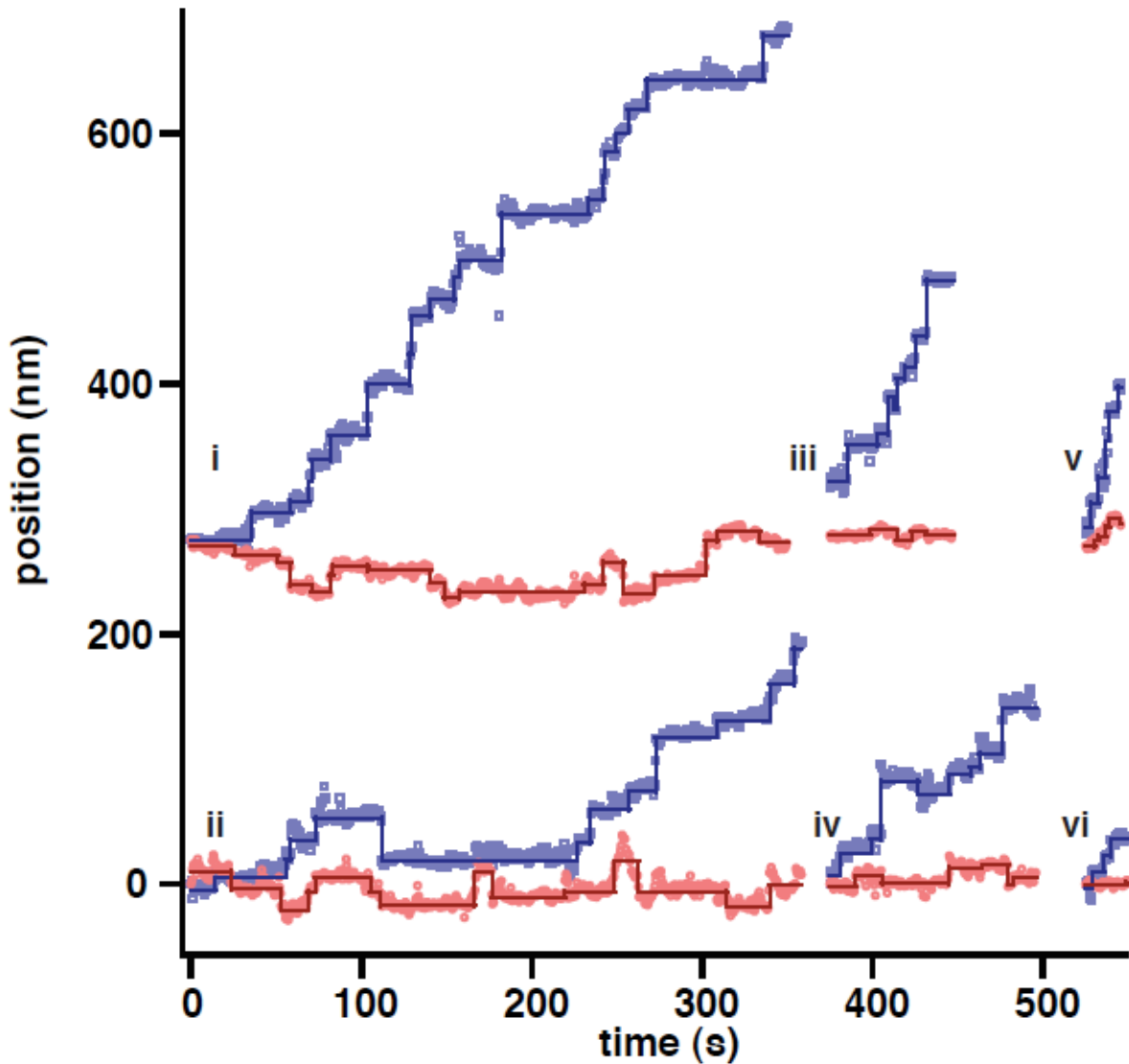


FIGURE S5 Myosin X takes side-to-side steps as it walks forward along a fascin-actin bundle. Gallery of example  $x$  position (*pale blue squares*) and  $y$  position (*pale red circles*) versus time for six example events of Qdot-labeled myosin X stepping along bundled actin. Each event is labeled near its beginning with a Roman numeral. The step-fitting algorithm of Kerssemakers et al. 2006 (2) was used to pick steps in  $x$  and  $y$  independently of each other (*dark blue and dark red traces*). Example trace (*i*) is the same event as in Fig. 1 *b* and *c* and Fig. 2 *a* for comparison.

Figure S6

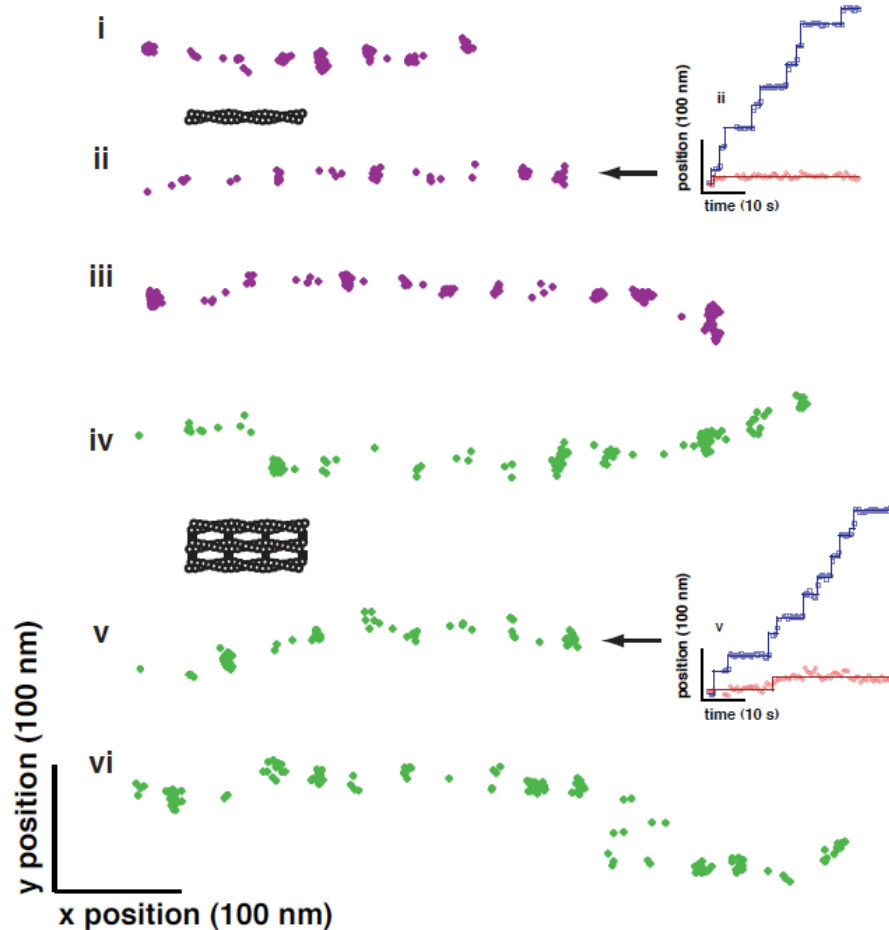


FIGURE S6 Myosin V demonstrates little side-to-side motion as it steps along actin filaments and actin bundles. Example  $x$  position versus  $y$  position traces of Qdot-labeled myosin V as it moves along single actin filaments (*violet, i-iii*) and along bundled actin (*green, iv-vi*). Each event is labeled near its beginning with a Roman numeral. Events are moving primarily in the positive  $x$  direction. (*insets*) Example traces of  $x$  position (*pale blue squares*) and  $y$  position (*pale red circles*) versus time for two of the example events of Qdot-labeled myosin V stepping along actin. The step-fitting algorithm of Kerssemakers et al. 2006 (2) was used to pick steps in  $x$  and  $y$  independently of each other (*dark blue and dark red traces*). Although some sideways transitions are detected on both architectures, sideways steps are a smaller proportion of the total detected steps (9% on single filaments and 6% on bundles;  $n = 265$  and 282 total steps, respectively) compared to myosin X stepping on bundles (36%). Fewer oblique steps (12% on single filaments and 10% on bundles) are observed for myosin V than for myosin X on bundles (22%). These differences between proportions is statistically significant when comparing myosin X on bundles to myosin V on either actin structure ( $p < 0.05$ , by two-proportion  $z$ -test). Additionally, the stepsize measurements for myosin V on both actin architectures from runlength traces ( $37.1 \pm 0.9$  nm on single filaments, mean  $\pm$  SE,  $n = 244$  steps from 12 motors;  $35.7 \pm 1.3$  nm on bundles, mean  $\pm$  SE,  $n = 252$  steps from 10 motors) and from  $x$  position traces ( $38.2 \pm 0.8$  nm on single filaments, mean  $\pm$  SE,  $n = 237$  steps;  $34.0 \pm 1.4$  nm on bundles, mean  $\pm$  SE,  $n = 240$ ) are in agreement with each other and with previous measurements on myosin V (4).



Figure S7

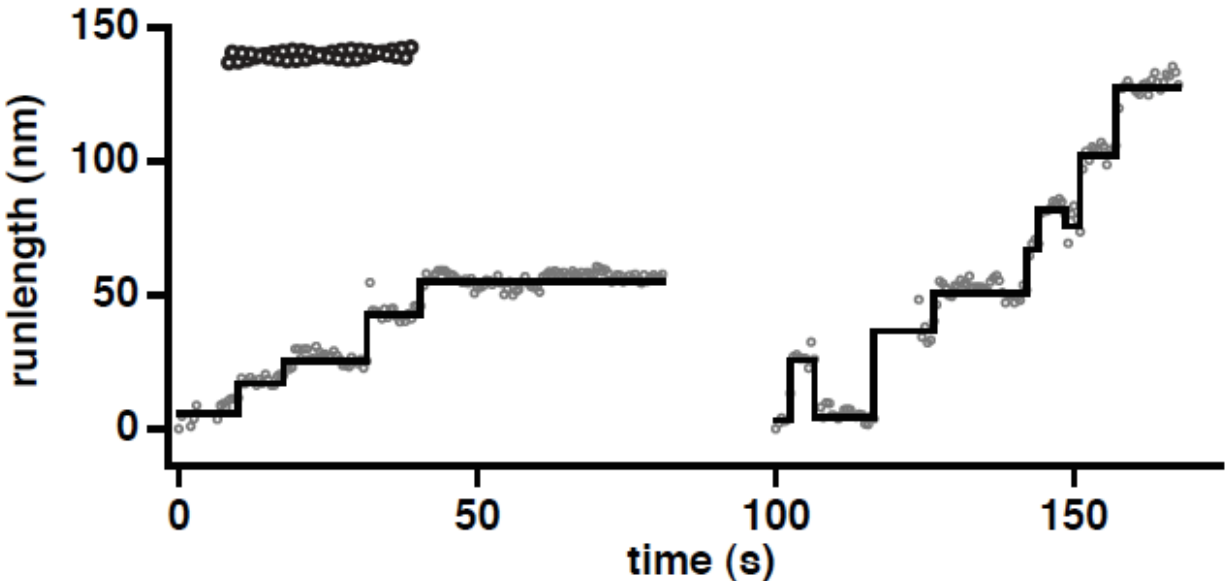


FIGURE S7 Myosin X steps short of 36 nm on single actin filaments. Plot of runlength over time (*gray circles*) for two example events. Steps (*black trace*) were picked from runlength traces using the step-fitting algorithm (2). The distribution of stepsizes is shown in Fig. 2 c.

Figure S8

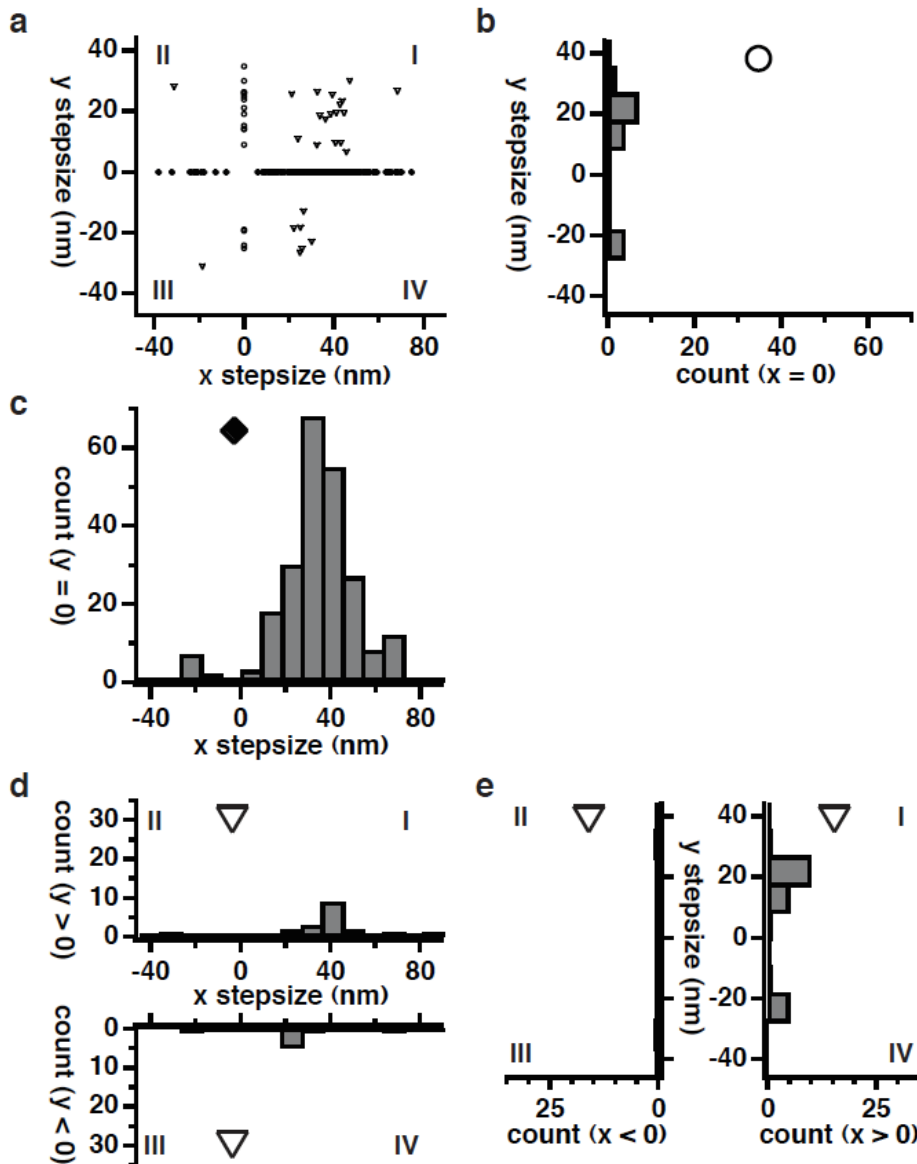


FIGURE S8 Myosin V walks along single filaments within a fascin-actin bundle. (a) Scatter plot of the  $x$  and  $y$  components for all steps on fascin-actin bundles ( $n = 282$ ). Steps occur either along the  $x$  axis (solid diamonds,  $n = 237$ ), along the  $y$  axis (open circles,  $n = 18$ ), or in one of the four Cartesian quadrants (open triangles,  $n = 27$ ). Quadrants are noted with Roman Numerals. (b) Histogram of  $y$  stepsizes with no corresponding  $x$  stepsize ( $n = 18$ ; 13 positive  $y$  stepsizes, 5 negative  $y$  stepsizes). (c) Histogram of  $x$  stepsizes with no corresponding  $y$  stepsize ( $n = 237$ ; 225 positive  $x$  stepsizes, 12 negative  $x$  stepsizes). (d) *Top*, histogram of  $x$  stepsizes of concurrent steps with a positive  $y$  stepsize ( $n = 19$ ; Quadrants I and II,  $n = 18$  and  $n = 1$ , respectively). *Bottom*, histogram of  $x$  stepsizes of concurrent steps with a negative  $y$  stepsize ( $n = 8$ ; Quadrants III and IV,  $n = 1$  and  $n = 7$ , respectively). (e) *Left*, histogram of  $y$  stepsizes of concurrent steps with a negative  $x$  stepsize ( $n = 2$ ; Quadrants II and III,  $n = 1$  and  $n = 1$ , respectively). *Right*, histogram of  $y$  stepsizes of concurrent steps with a positive  $x$  stepsize ( $n = 25$ ; Quadrants I and IV,  $n = 18$  and  $n = 7$ , respectively). Note that the motor takes very few sideways or oblique steps compared to steps along the  $x$ -axis.

Figure S9

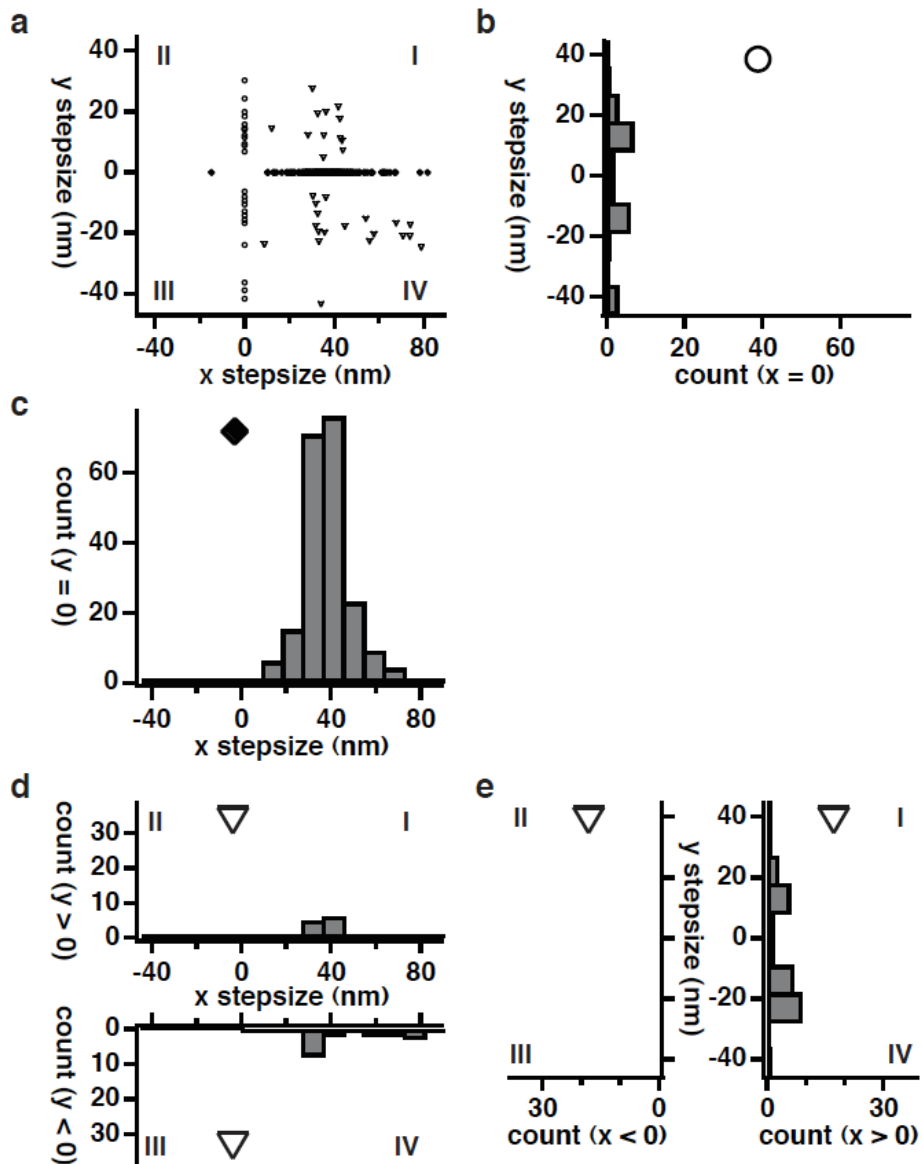


FIGURE S9 Myosin V steps mostly straight along surface-attached actin filaments. (a) Scatter plot of the  $x$  and  $y$  components for all steps on single actin filaments ( $n = 265$ ). Steps occur either along the  $x$  axis (solid diamonds,  $n = 207$ ), along the  $y$  axis (open circles,  $n = 25$ ), or in one of the four Cartesian quadrants (open triangles,  $n = 33$ ). Quadrants are noted with Roman Numerals. (b) Histogram of  $y$  stepsizes with no corresponding  $x$  stepsize ( $n = 25$ ; 13 positive  $y$  stepsizes, 12 negative  $y$  stepsizes). (c) Histogram of  $x$  stepsizes with no corresponding  $y$  stepsize ( $n = 207$ ; 206 positive  $x$  stepsizes, 1 negative  $x$  stepsize). (d) *Top*, histogram of  $x$  stepsizes of concurrent steps with a positive  $y$  stepsize ( $n = 13$ ; all in Quadrant I). *Bottom*, histogram of  $x$  stepsizes of concurrent steps with a negative  $y$  stepsize ( $n = 20$ ; all in Quadrant IV). (e) *Left*, No  $y$  stepsizes for concurrent steps with a negative  $x$  stepsize were detected. *Right*, histogram of  $y$  stepsizes of concurrent steps with a positive  $x$  stepsize ( $n = 33$ ; Quadrants I and IV,  $n = 13$  and  $n = 20$ , respectively). Note that the motor takes very few sideways or oblique steps compared to steps along the  $x$ -axis.

Figure S10

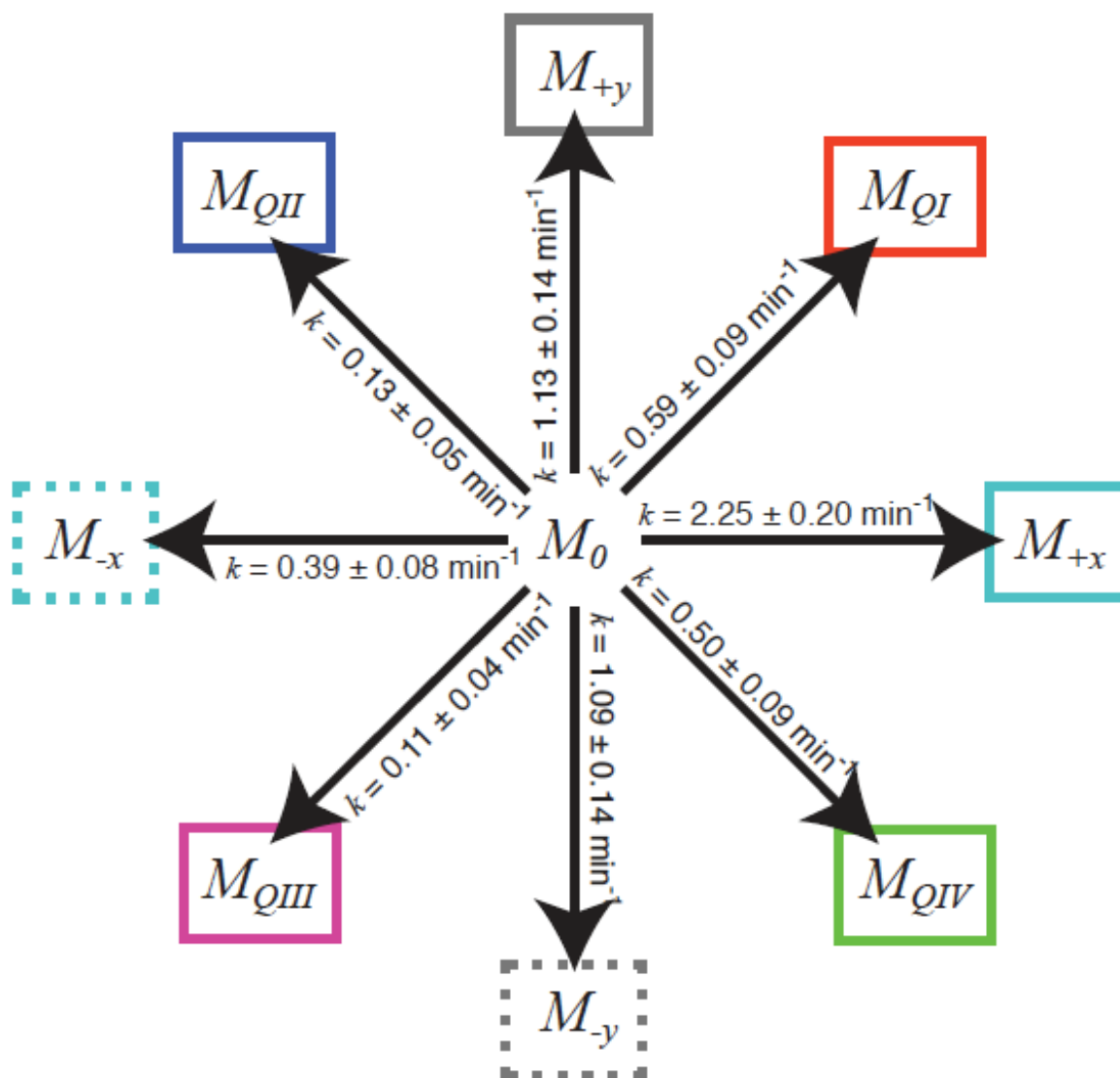
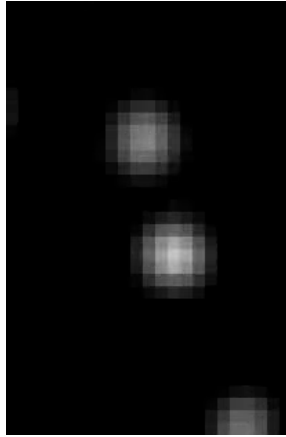


FIGURE S10 Kinetic scheme of observed rates of myosin X stepping in all directions on a fascin-actin bundle. From the mean dwelltime (see Fig. 5), the overall observed stepping rate for myosin X under the experimental conditions was found to be  $6.20 \pm 0.38 \text{ min}^{-1}$  (mean  $\pm$  SE). Because the dwelltime distribution does not change no matter which direction the motor steps, each direction of stepping is a competing pathway exiting from a common intermediate (5). Thus, the rate of stepping in any given direction is the product of the overall stepping rate and the fraction of steps occurring in that direction. In the scheme, on-axis steps are categorized as being along the positive x axis, the negative x axis, the positive y axis, or the negative y axis. Oblique steps are categorized into Cartesian quadrants I, II, III, and IV (as in Fig. 4). The colored boxes correspond to the color of the dwell time distributions for each type of step in Fig. 5.

## Movie S1



MOVIE S1 Myosin X takes sidesteps as it walks along a fascin-actin bundle. Example movie of quantum dot-labeled myosin X stepping slowly along a fascin-actin bundle. The first eight frames of the movie show an image of the ATTO-647N phalloidin fascinactin bundle. The motor is walking predominantly from the upper left to the lower right of the frame, with sidesteps visible to the observer's left and right. Image height 3.28  $\mu\text{m}$ , image width 1.43  $\mu\text{m}$ , exposure 0.5 s/frame, playback 60 frames/s.

## Supporting Information References

1. Meijering, E., M. Jacob, J. C. Sarria, P. Steiner, H. Hirling, and M. Unser. 2004. Design and validation of a tool for neurite tracing and analysis in fluorescence microscopy images. *Cytometry A* 58:167-176.
2. Kerssemakers, J. W., E. L. Munteanu, L. Laan, T. L. Noetzel, M. E. Janson, and M. Dogterom. 2006. Assembly dynamics of microtubules at molecular resolution. *Nature* 442:709-712.
3. Yildiz, A., J. N. Forkey, S. A. McKinney, T. Ha, Y. E. Goldman, and P. R. Selvin. 2003. Myosin V walks hand-over-hand: single fluorophore imaging with 1.5-nm localization. *Science* 300:2061-2065.
4. Mehta, A. D., R. S. Rock, M. Rief, J. A. Spudich, M. S. Mooseker, and R. E. Cheney. 1999. Myosin-V is a processive actin-based motor. *Nature* 400:590-593.
5. Kolomeisky, A. B., E. B. Stukalin, and A. A. Popov. 2005. Understanding mechanochemical coupling in kinesins using first-passage-time processes. *Phys Rev E Stat Nonlin Soft Matter Phys* 71:031902.